Experimental investigation of the infrared extinction limitations for vapor concentration measurement in a gas/particle flow

V. Bodoc, D. Voicu

Experimental investigation of the infrared extinction limitations for vapor concentration measurement in a gas/particle flow.

Bodoc Virginel[1], Voicu Daniela[1]
[1] ONERA, 2 avenue Eduard Belin, 31055 Toulouse, FRANCE
* correspondent author : virginel.bodoc@onera.fr

Abstract A two-wavelength Infrared Absorption technique is applied on a gas/particle flow to investigate its behaviour in a reduced-scale environment. First, a brief introduction in the theory of Infrared absorption is done and the experimental setup is presented. Then, the results are presented and discussed for different scenarios. The reported results prove the general aptitude of the technique to be applied in the presence of particles of different concentration and sizes. The sources of error are analyzed and solutions to refine the results are presented.

1. Introduction

The interest to develop measurement techniques for the characterization of fuel sprays in reactive or non-reactive conditions has two main sources. On one hand it is compulsory to understand and control the effects, often dangerous, of the fuels used in risk areas such as: turbojets, industrial facilities, airports, etc. On the other hand it is the need of data useful in technological development corresponding to the fuel behavior in the combustion chambers. In this case the experimental results can be used directly for the design of new geometries of combustors or for the comparison with the numerical simulations.

For a gas-particle two-phase flow different measurement technique are available to investigate the behavior of each phase. Hence, non-intrusive methods, based on the use of laser beams allow to get the droplet's velocity (Laser Doppler Anemometry - LDA, Particle Image Velocimetry - PIV), size (Phase Doppler Anemometry – PDA and Malvern), temperature and composition (Laser Induced Fluorescence – LIF and Rainbow Refractometry). All these techniques are based on the diffusion of light by transparent droplets or on the fluorescent properties of the liquid components.

To determine the velocity field of the continuous phase the LDA and PIV may also be used with small particles as tracers. The composition and the temperature of the continuous phase are nowadays obtained mainly by LIF. The successful application of this technique implies the mobilization of important material resources such as tunable lasers and intensified cameras. If the technique largely proved its capacity to provide reliable results for a wide range of configurations, its temporal resolution limitations makes it suitable basically for steady flow. Moreover, because of the sensitivity towards concentration gradients, its application for two-phase configuration is limited.

A possible solution to overcome these limitations is based on the utilisation of absorption properties of the continuous phase. The use of optical measurement techniques based on the infrared radiation absorption by hydrocarbon molecules may be traced back in the early 80s. Since, an important number of publications have dealt with the application of such techniques to measure the concentration of vapours in different configurations. The efficiency and accuracy of such techniques were widely proved for monophase flows [1], [2], [3], [4] most often in the presence of a single chemical species

Nevertheless, for two-phase flows the reported results are still incomplete. Hence, the results published in [5], [6], [7], [8] were obtained for a limited number of gas concentrations, particles mass loadings and particle sizes. This makes it difficult to identify the technique limitations for real applications such as aeronautic combustors for example.

Within this work, the objective is to provide a step forward in the investigation of the limitations of the infrared extinction technique when is applied to a two-phase flow. This work

represents also a first step in the investigation of a more complex configurations as multiphase flow inside aeronautical combustion chambers.

This paper is organised as follows. Section 2 introduces the principles of the measurement technique applied to a two-phase flow. In the third part the experimental bench is described and the optical set-up is detailed. In the forth section of the paper the results are presented and discussed for pure gaseous phase, for pure dispersed phase and for a two-phase flow.

2. Description of the measurement technique.

The extinction (absorption and scattering) of a laser beam intensity after crossing a medium with randomly distributed particles is theoretically described by Bouguer-Lambert-Beer (BLB) law that was derived from laser beam energy conservation [10]:

$$\frac{I}{I_0} = \exp(-\tau) = \exp\left[-\overline{C}_n \cdot L \cdot \frac{\pi}{4} \cdot \int_0^{\infty} Q_{ext}(\lambda, n, D) \cdot D^2 \cdot N(D) dD\right] \qquad \textbf{Equation 1}$$

$$Q_{ext}(\lambda, n, D) = Q_{scat}(\lambda, n, D) + Q_{abs}(\lambda, n, D)$$

in which τ is defined as the optical thickness of the medium. Q_{sca} and Q_{abs} are the scattering and absorption efficiencies factors depending on the light wavelength (λ), size of particles (D), and the complex refractive index (n). $\overline{C}_n$ and N(D) are the particles mean density number and the diameter distribution respectively.

If the continuous phase is absorbent, the previous equation becomes:

$$\frac{I}{I_0} = \exp(-\tau) \cdot \exp[-\alpha \cdot \bar{c} \cdot L] \qquad \textbf{Equation 2}$$

where $\bar{c}$ represents the mean molar concentration, α is the molar absorption coefficient of the medium and L the geometrical path.

The Infrared Absorption (AIR) technique is based on the simultaneous measurement of laser beam extinction for two wavelengths λ_1 and λ_2.

The value of λ_1 is selected in order to allow an important absorption in the continuous phase. Usually the hydrocarbons show such a behaviour for infrared radiation. On the contrary, λ_2 is chosen such that it does not undergo any absorption in the continuous phase. For practical reasons (availability of the laser sources and important absorption coefficients) most of the optical arrangements were developed for $\lambda_1 = 3.39\,\mu m$ and $\lambda_2 = 0.632\,\mu m$.

From the measured extinctions, the mean molar concentration is obtained from Equation 1 and Equation 2 with the formula:

$$c = \frac{1}{\alpha \cdot L}\left[-\tau_1 - \ln\left(\frac{I}{I_0}\right)_{\lambda_1}\right] = \frac{1}{\alpha \cdot L}\left[\ln\left(\frac{I}{I_0}\right)_{\lambda_2}\frac{\tau_1}{\tau_2} - \ln\left(\frac{I}{I_0}\right)_{\lambda_1}\right] =$$

$$= \frac{1}{\alpha \cdot L}\left[\ln\left(\frac{I}{I_0}\right)_{\lambda_2}\frac{Q_{ext}(\lambda_1, n, D)}{Q_{ext}(\lambda_2, n, D)} - \ln\left(\frac{I}{I_0}\right)_{\lambda_1}\right] \qquad \textbf{Equation 3}$$

This equation implies that the extinction efficiencies ratio $\frac{Q_{ext}(\lambda_1, n, D)}{Q_{ext}(\lambda_2, n, D)}$ is previously known. Different investigations based on the simulation of light diffusion within the Mie theory [7] have shown that the extinction efficiencies ratio may be assumed being equal to 1 independently of the refractive indices of droplets if the area mean drop diameter is $D_{20} > 20\mu m$.

In practical applications there are some other difficulties in the application of Equation 3 to deduce the mean molar concentration. Hence, following van Hulst [10], a detector measuring the laser beamt intensity after crossing a gas/particle flow, « sees » simultaneously the attenuated energy of source and scattered light in its field of view (FOV). This effect is more important for large spheres because the scattered light is more concentrated near the forward direction. The effect of the FOV of the detector on the received intensity of a laser beam undergoing multiple scattering was numerically performed by A. Zardecki at al. [13].

The limits of BLB law were experimentally tested by N. L. Swanson et al. [12] using a 514.5 nm laser. The authors assumed that the radiant intensity measured after light crosses the medium cannot neglect the scattered light by particles. This effect is more obvious for high values of the optical thickness and particles size. Nevertheless, limiting the FOV of the detector the amount of the scattered light reaching the sensor may be limited. In these conditions the BLB law was proved to be valid for dense media ($\tau < 10$) if the FOV half-angle satisfies the so called the Hodkinson criterion: $\theta_{1/2} < 7° \cdot \frac{\lambda}{d}$ where λ corresponds to the wavelength of the radiation and d to the diameter of droplets. As shown by G. Gouesbet et al [14] this condition, demonstrated for single scattering particles, is expected to remain sufficient if the multiple scattering is accounted.

2. Materials and methods

The test channel, presented in Fig. 1, provides the two-phase flow conditions for the study of the measurement technique. It allows the simultaneous introduction of the premixed nitrogen, ethanol vapor and transparent glass particles. The ethanol mole fraction is controlled by means of an evaporating system which was developed within the PhD thesis of Wagner [9]. Its master component is the Bronkhorst W-202A Controlled Evaporation Mixer (CEM). This device allows to obtain fuel vapor at defined fractions from 0 to 100 % and temperatures up to 200 °C. The ensemble of flow meters and CEM is PC controlled. As main process gas the nitrogen was chosen because of its chemically inert behavior. The spherical and transparent glass particles simulating fuel droplets are introduced using a Lambda powder dosing device. It allows to introduce well established amounts of particles in the channel. To investigate the influence of the particles diameter on the technique accuracy, particles with different size distributions were used.

The gas and particles injection is performed using a well defined procedure that is repeated identically for each experimental run.

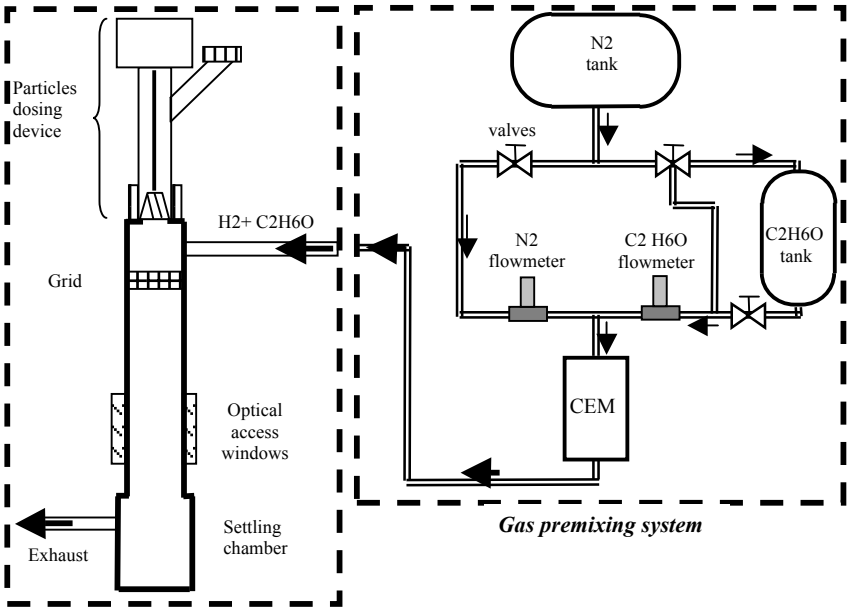

Fig. 1. Two-phase flow test section

The optical set-up is presented in Fig. 1. Two laser light sources of 632 nm and 3.39 μm are employed. The two laser beams are centered using a semitransparent mirror. A tunable chopper (1-6 kHz) produces a time dependent signal which is used as trigger source by the acquisition system. After crossing the probe volume the laser's beam intensity is detected by photo diodes. The visible detector is a Si-type photodiode while the amount of infrared radiation is measured by a PbSe photoconductive detector. To minimize thermal noise the IR detector is embedded in a thermoelectric heat sink which regulates the operating temperature. To increase their dynamics, the two detectors are connected to pre-amplifying lock-in circuits. The conditioning and storage of the pre-amplified signals are ensured by an acquisition system from National Instruments that is controlled by a Labview-based application.

The IR receiver is protected by a ND filter with an optical density of 0.3 to set the detector at a correct operating point. In this way the overexposure of the sensitive element is avoided.

During acquisitions it was observed that the ND filter used to control the intensity of the IR beam may reflect backward an amount of the light intensity. Following the laser producer, the back reflections into the laser cavity will impair the ability of the electronics to stabilize the intensity of the laser [15]. To avoid this effect, the filter was not placed perpendicularly on the direction of the laser beam. Taking this precaution, the drift of the laser beam was kept at relatively law values.

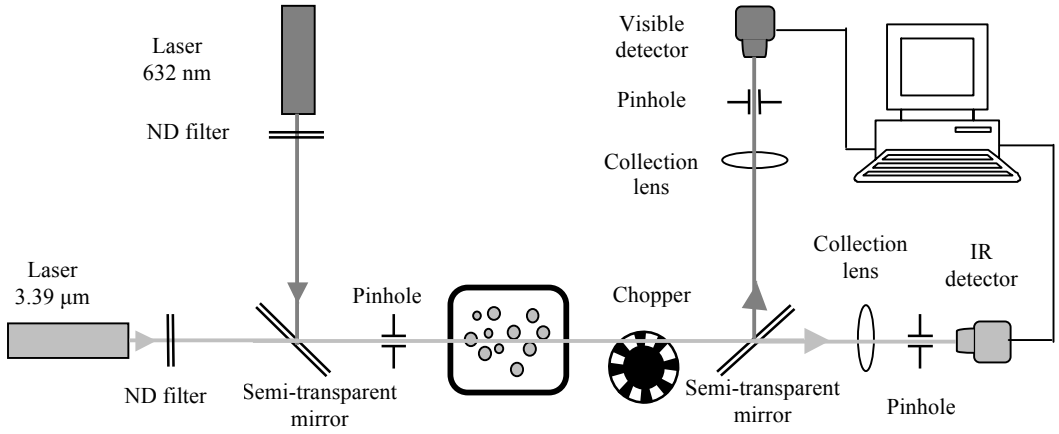

Fig. 2. Optical experimental set-up

The alignment of the laser beams was realized with the "razor blade" technique.

As it was presented before, it is theoretically possible to express the extinction of light from a point source using the BLB law. Nevertheless, in practice the detectors measure the attenuated light of the source plus a certain amount of light scattered at small angles. These angles are defined by the FOV of the detector. For the optical setup presented here the amount of the scattered light seen by the detectors has been minimized by placing lens-pinhole assemblies before the detectors. The characteristics of these components are listed in Table 1.

Table 1. Characteristics of the lens-pinholes assemblies.

	$\lambda_1=3.39\mu m$	$\lambda_2=0.632\mu m$
Lens focal length [mm] f	50	100
Pinhole size [mm] r	0.4	0.15
Field of View half angle [degrees]	0.229	0.043

Using the values from this table it presents a real interest to check the applicability of the Hodkinson criterion for this experimental setup. Fig. 3 plots for the two wavelengths the limits of

the FOV as defined by the Hodkinson criterion for different sizes of droplets. The same graph presents the FOVs of the optical arrangement as calculated with the elements from Table 1. It can be observed that the amount of scattered light entering in the detector may be considered as negligible for droplets inferior to 100 μm in diameter both for visible and infrared radiation.

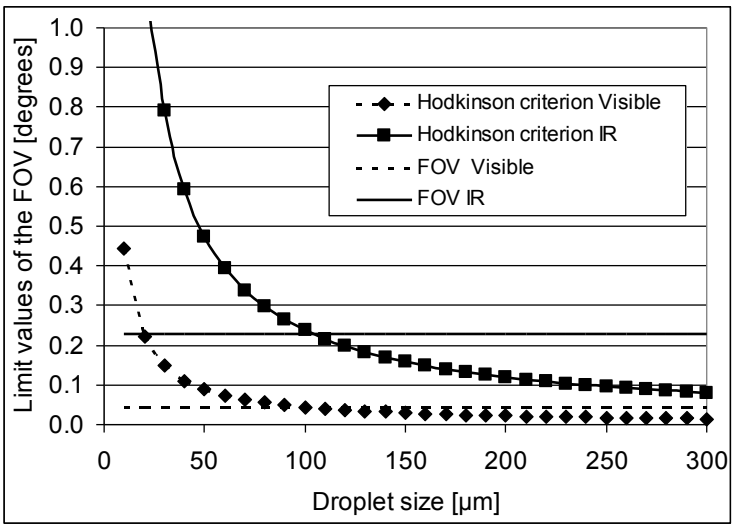

Fig. 3. Evolution of the Field of View limits with the droplet size for the two wavelengths.

Moreover, from the values in the Table 1 it may be observed that the ratio $r/(\lambda \cdot f)$ is kept constant for both the infrared and visible transmission measurements. From the theory describing the light diffusion by transparent spheres it results that the same amount of scattered light will enter the detectors [8, 10] without no influence on the extinction efficiencies ratio from Equation 3 .

With this optical set-up the reference beams intensities I_0 and attenuations cannot be measured simultaneously. The solution consists in the measurement of the incident laser beam intensities before any measurement of the attenuation through the medium. These measurements were performed systematically in order to check that the temporal drift of the lasers is minimal. It was observed that this condition was satisfied after at least 30 minutes from the lasers switching-on.

To overcome the problems related to the variation of the particle density number in time, the measurements were performed for the two wavelengths simultaneously.

3. Results

3.1. Results obtained for the pure gaseous phase

In a first stage the measurements were performed for the pure gaseous phase at different temperatures. The measurements were performed using a calibration cell instead the test channel from ***Fig. 1***. The calibration cell was used because it allows an accurate control of the temperature of the gas in the range of 20-200°C. The operating conditions are listed in Table 2. The concentration of the ethanol in the cell test was successively increased.

Table 2. Operating conditions for the pure gaseous flow.

Flow rate N_2	7	ln/min
Temperature in the cell	70	°C
Acquisition frequency	10000	Hz

Acquisition period	3	s

Fig. 4plots the measured vapor mol fractions against the input value. The abscise corresponds to the molar fractions of the ethanol vapors introduced in the test channel. The ordinate corresponds to the molar fraction measured with the AIR technique. The continuous black line represents the expected values of the measurement. The measured values (circle symbols on the graph) were obtained taking into account a molar absorption coefficient (decade value) $\alpha = 3.2\ m^2/mol$. The slope of the line is equal to 1, which shows that there is almost no difference between the real and the measured values. The mean differences between the two series of data are between ±0.11 % in absolute units which is equivalent to a relative uncertainty of 1.3% for a measured value of 8.69 % molar fraction of ethanol. Among the different sources of uncertainty it was observed that the temporal drift of the laser beam intensity plays a dominant role.

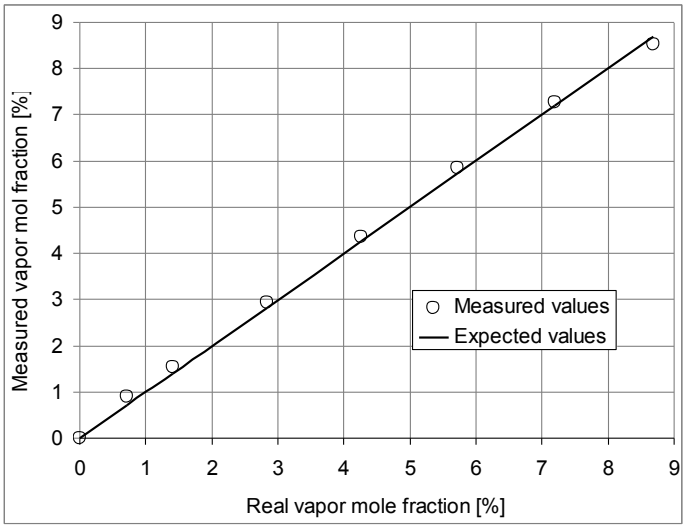

Fig. 4. The vapor mole fraction measured in the cell without particles.

In the following it is assumed that the molar absorption coefficient of the ethanol is unknown and it is estimated by fitting the measured values of the vapor mol fraction with the input values. The results obtained for different temperatures of the gas are shown in Fig. 5 and are compared with the values published in literature. It may be observed that the values of the absorption coefficient obtained in this way are very close to those previously reported by Tsuboi [1] and Mevel [3].

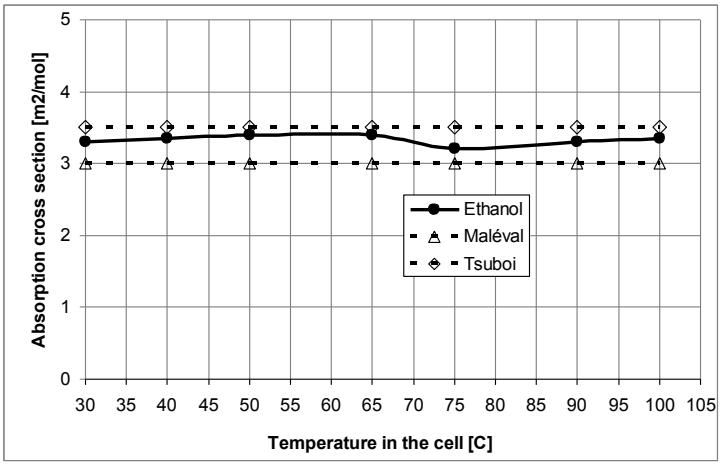

Fig. 5. The temperature dependence of the ethanol decade absorption coefficient.

3.2. Results obtained for pure dispersed phase.

Before the application of the AIR technique to measure the concentration of ethanol vapors in the presence of dispersed phase, it presents a real interest to analyse the scattering of light by the glass particles in a non-absorbing nitrogen medium. The tests were done for well controlled amounts of glass particles of three different sizes. In a first step, the size and velocity of the particles crossing the probe volume were characterized using a PDA equipment from DANTEC. The size and velocity distributions for the three types of particles used in this study are presented in Fig. 6 and Fig. 7 These values will be used further on to calculate the concentration of particles in the channel. From now on in this paper the three distribution will be denominated as: D1 (D_d=10-100 μm), D2 (D_d=50-170 μm) et D3 (D_d=160-280 μm).

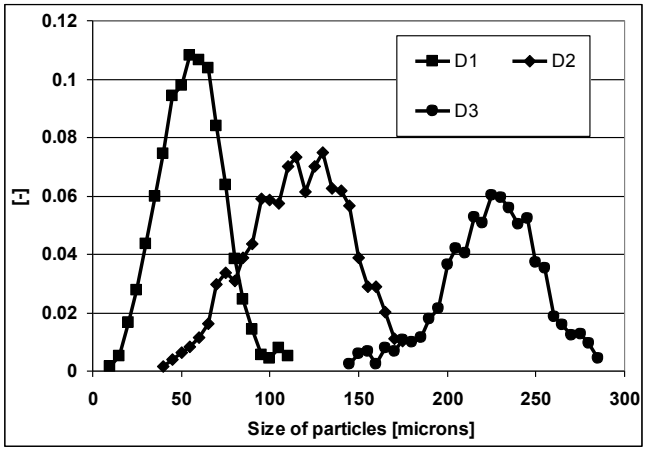

Fig. 6. Size distribution measured by PDA

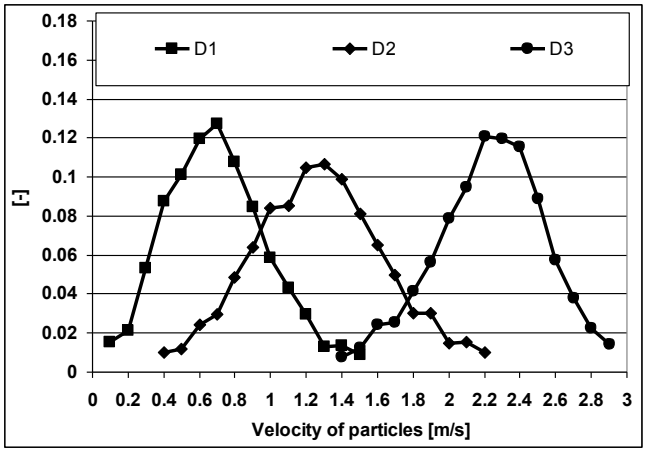

Fig. 7. Velocity distribution measured by PDA.

With the glass particles hence characterised, the beam attenuation was measured simultaneously for both wavelengths. The results obtained are plotted in Fig. 8, Fig. 9 and Fig. 10. In these figures, the ordinate corresponds to measured optical depth defined as $\tau = \ln\left(\frac{I_0}{I}\right)$.

The values of this quantity may also be obtained analytically using the Equation 1 [12]:

$$\tau = \overline{C}_n \cdot L \cdot \frac{\pi}{4} \cdot \int_0^\infty Q_{ext}(\lambda, n, D) \cdot D^2 \cdot N(D) dD = \overline{C}_n \cdot L \cdot \overline{Q}_{ext} \cdot \frac{\pi}{4} \cdot \int_0^\infty D^2 \cdot N(D) dD =$$
$$= \overline{C}_n \cdot L \cdot \overline{Q}_{ext} \cdot \sigma_{geom} \qquad \textbf{Equation 4}$$

where σ_{geom} represents the geometric cross section of particles.

If in Fig. 8, Fig. 9 and Fig. 10 the abscise corresponds to the product $\overline{C}_n \cdot \sigma_{geom} \cdot L$, the experimental extinction efficiency may be calculated as the slope of the tendency line. The particle mean density number was determined from the mass rate of particles introduced in the channel and their velocity in the probe volume.

The values of the mean experimental extinction efficiency $\overline{Q}_{ext}$ are shown on each graph for the two wavelengths and the three types of particles. Their comparison with theoretical values (Q_{Mie}= 2.1±0.1 for particles with a diameter superior to 20 μm) presents a real interest .

Hence, for small particles (D1 type) there are practically no differences between the extinction efficiencies measured experimentally for visible and infrared radiation and the theoretical value. Nevertheless, the same comparison for larger particles (D2 and D3 types) shows unexpected differences which increase with the size of droplets. Hence, if the $\overline{Q}_{ext}$ measured for the infrared radiation is very closed to the theoretical value, the same behaviour is not obtained for the visible beam. For the two size distribution, the most important observation is that the extinction efficiencies ratio is different from 1 which makes impossible the application of Equation 3.

An explanation of this result may be provided by the optical arrangement. Hence, for yet unknown reasons the optical similarity for the two wavelengths detectors is not achieved. In these conditions, the particles with diameters superior to 100μm are expected to scatter important and different amounts of radiation to the detectors surface.

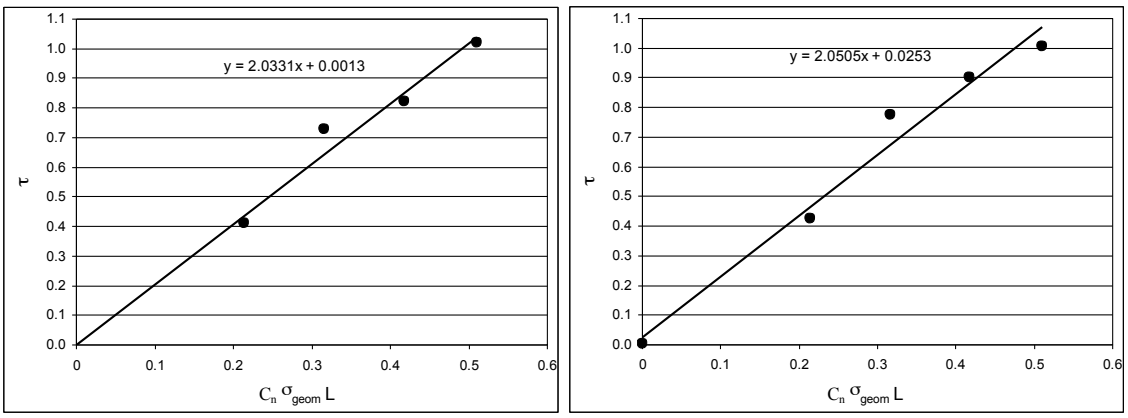

Fig. 8. Optical thickness of particles measured for λ= 632 nm (left side image) and λ= 3.39 μm (right side image) for D1 type particles.

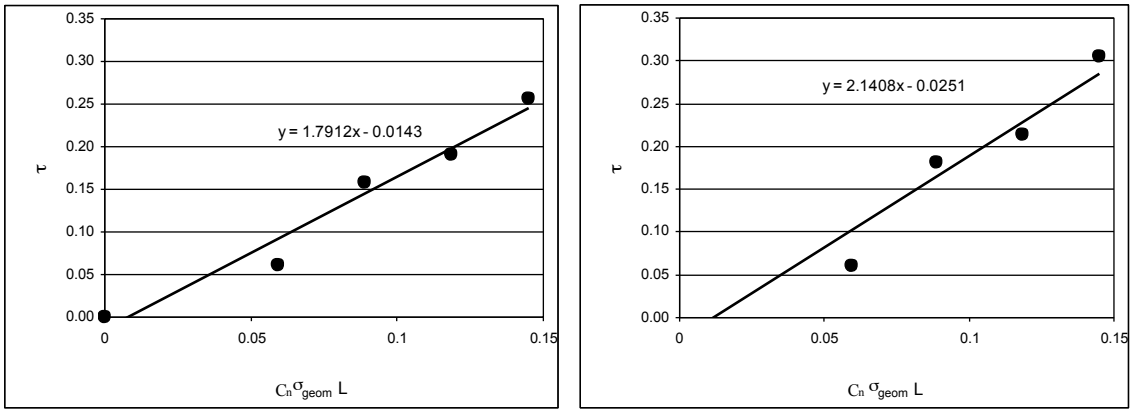

Fig. 9. Optical thickness of particles measured for λ= 632 nm (left side image) and λ= 3.39 μm (right side image)for D2 type particles

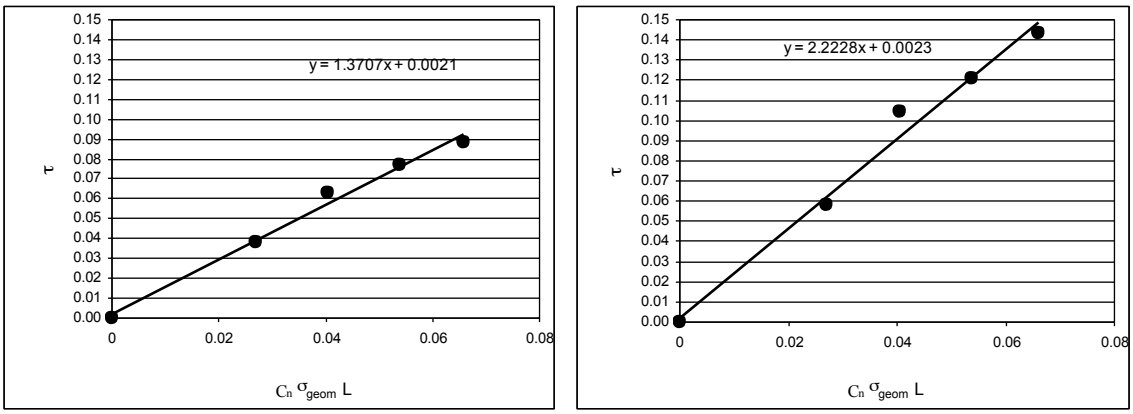

Fig. 10. Optical thickness of particles measured for λ= 632 nm (left side image) and λ= 3.39 μm (right side image) for D3 type particles

3.3. Results of the vapour concentration measured in the presence of transparent particles.

Fig. 11, Fig. 12 and Fig. 13 presents the concentrations of ethanol vapours measured in the presence of glass particles. The values of the mole fractions were obtained using the Equation 3 and assuming a value of 1 for the extinction efficiencies ratio. On the same graph were plotted the values obtained for different volume fractions $c_1 - c_5$ of the dispersed phase.

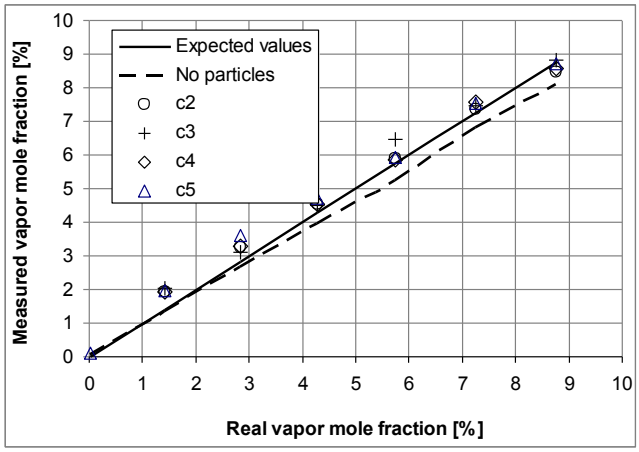

Fig. 11. Values of the vapour concentration measured in the presence of D1 type particles (c_2=1.64e-4, c_3=2.42e-4, c_4=3.2e-4, c_5=3.9e-4).

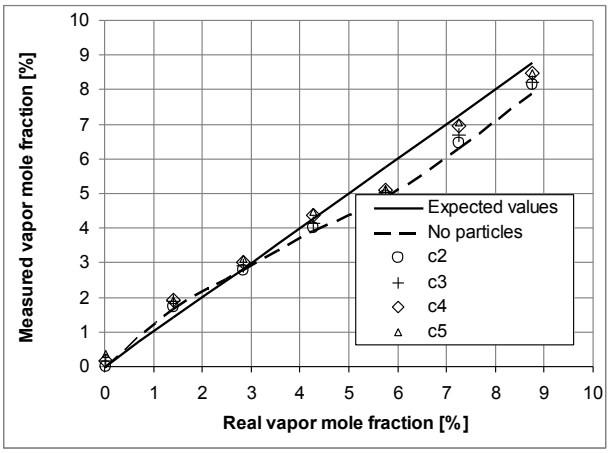

Fig. 12. Values of the vapour concentration measured in the presence of D2 type particles (c_2=7.28e-5, c_3=1.09e-4, c_4=1.45e-4, c_5=1.78e-4).

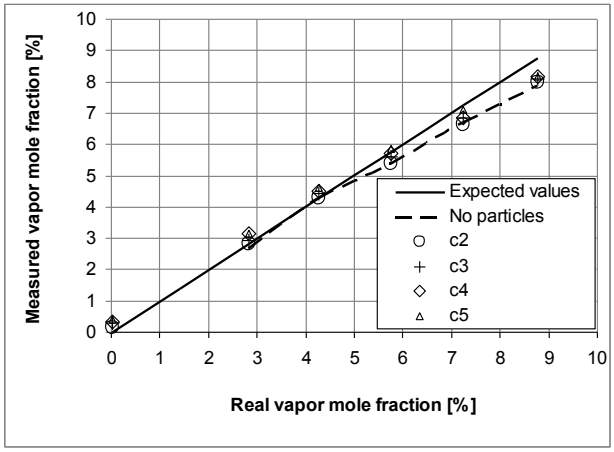

Fig. 13. Values of the vapour concentration measured in the presence of D3 type particles (c_2=4.16e-5, c_3=6.24e-5, c_4=8.32e-5, c_5=1.02e-4).

The results show that the measurement technique may be applied successfully for different concentrations of particles and vapours of ethanol. Using the particle distribution system, volume fractions of particles up to 0.0004 may be reached corresponding rather to dilute sprays.

It is found that the variation of the droplets' concentration does not influence on the measured values of the vapour mole fractions, the differences between the different series of data being inferior to 0.2÷0.3% in absolute units. Nevertheless, some differences are obtained with respect to the input values. An explication of these errors, which are more visible for D2 and D3 type particles, may be found in the adopted value of the extinction efficiencies ratio that is quite different by the measured one in paragraph 3.3. However, the law level of particles concentration may explain why in this case the measurement errors are relatively reduced.

4. Conclusions.

The purpose of this paper is to provide a systematic investigation of the Infrared Absorption technique in the perspective of its application to real aeronautical sprays in evaporation. The approach applied consists in the reproduction of different two-phase flow conditions. That was possible by variation of different parameters such as: the gas molar

concentration, the particle number density and particle sizes. If for the pure gaseous phase the results fully agree with the literature data, some differences are observed in the presence of a dispersed phase.

The results obtained demonstrate the feasibility of the Infrared Absorption technique to provide enough accurate results (errors inferior to 10%) on the concentration of fuel vapours in the presence of polydispers clouds of transparent particles with diameters between 10-280 μm. Nevertheless, the precision of measurement was demonstrated only for low dense media. Following the results, to extend the application of the same optical setup to dense sprays, the couples pinholes-lenses placed in front of the detector must be reviewed.

Bibliography

1. T. Tsuboi et al. – Light absorption by hydrocarbon molecules at 3.392 μm of He-Ne laser, Japanese Journal of Applied Physics, vol. 24, No. 1, pp. 8-13, 1985.
2. J. Drallmeier – Hydrocarbon absorption coefficients at the 3.39 μm He-Ne laser transition, Applied Optics 42 (6) (2003) 979-982
3. R. Mevel et al – Absorption cross section at 3.39 μm of alkanes, aromatics and substituted hydrocarbons, Chemical Physics Letters 2012
4. B. Gillet et al. – Infrared absorption for measurement of degree of premixedness of hydrocarbon fuel/air mixtures, Proceedings of the European Combustion Meeting, 2003
5. M. Adachi et al. – Non-intrusive measurement of gaseous species in reacting and non-reacting sprays, Combustion Science and Technology, vol. 75, pp. 179-194, 1991.
6. J.A. Drallmeier and J.E. Peters – Experimental investigation of fuel spray vapor phase caracterisation, Atomization and Sprays, vol 1, pp. 63-88, 1991
7. J. Drallmeier, - Hydrocarbon vapor measurements in fuel sprays: a simplification of the infrared extinction technique, Applied Optics, vol. 33, No.30, pp. 7175–7179, 1994.
8. T.P. Billings and J. A. Drallmeier, A detailed assessment of the infrared extinction technique for hydrocarbon vapor measurements in a controlled two-phase flow, Atomization and sprays, vol. 4, pp. 99-121, 1994
9. B. Wagner - Fuel vapor concentration measurements on droplets by Infrared Extinction, PhD thesis University of Toulouse, 2009
10. H. C. van de Hulst – Light Scattering by Small Particles, Dover publication, Inc, New York, 1981
11. T. G. Ellestad – A diffraction technique to measure size distribution of large airborne particles
12. N. L. Swanson – Limits of optical transmission measurements with application to particle sizing techniques, Applied Optics, vol. 38, No. 27, 1999
13. A. Zardecki and A. Deepak – Forward multiple scattering corrections as a function of detector field of view, Applied Optics, vol. 22, No. 19, 1983
14. G. Gouesbet et al – Visible infrared double extinction measurement in densely laden media, Proceedings of an international symposium on optical particle sizing, 1987, Rouen, France
15. www.thorlabs.de